Electronic supplementary materials *Mendeleev Commun.*, 2025, **35**, 142–144

New tricyclic cage compound as allosteric modulator of the glutamatergic system: synthesis and biological activity

Elena A. Golubeva, Mstislav I. Lavrov, Polina N. Veremeeva, James Matthews, Eugene V. Radchenko, Vladimir L. Zamoyski, Vladimir V. Grigoriev and Vladimir A. Palyulin

Contents

1. Chemistry

NMR spectra were recorded on the Agilent 400-MR spectrometer (400.0 MHz for ^{1}H; 100.6 MHz for ^{13}C) at room temperature; chemical shifts (δ) were measured with reference to the solvents: $CDCl_3$ for ^{1}H (δ = 7.26 ppm), ^{13}C (δ = 77.16 ppm), DMSO-d_6 for ^{1}H (δ = 2.50 ppm), ^{13}C (δ = 39.50 ppm) and CD_3OD for ^{1}H (δ = 3.31 ppm), ^{13}C (δ = 49.00 ppm). Chemical shifts (δ) are given in ppm; *J* values are given in Hz. When necessary, assignments of signals in NMR spectra were made using 2D techniques. Accurate molecular mass measurements (HRMS) were performed on a Bruker micrOTOF II instrument using electrospray ionization (ESI). The measurements were done in a positive ion mode (interface capillary voltage 4500 V). Analytical thin layer chromatography was carried out with Merck Silica Gel 60 plates (supported on aluminum); the detection was done by UV lamp (254 and 365 nm) and chemical staining (solution of ninhydrin in EtOH). Column chromatography was performed on Merck Silica Gel 60.

*2-Amino-N-(5-cyanoindan-2-yl)-4-methoxybenzamide (**4**).* A mixture of 2-amino-4-methoxybenzoic acid **3** (212 mg, 1.27 mmol) and carbonyldiimidazole (226 mg, 1.39 mmol) in abs. acetonitrile (25 mL) was stirred for 6 hours until the imidazolide was formed (control by TLC). Then, a solution of 2-aminoindane-5-carbonitrile **2** (198 mg, 1.25 mmol) in abs. acetonitrile (6 mL) was added, and the reaction mixture was stirred at 50 °C for 14 hours until the initial amine disappeared (control by TLC, R_f = 0.07 in the $CHCl_3$/EtOH (20:1) system). After that, the solvent was distilled off. The resulting product was purified by column chromatography (eluents $CHCl_3$, $CHCl_3$/EtOH (100:1) and $CHCl_3$/EtOH (50:1)). This yielded 317 mg (1.03 mmol, 82%) of pure 2-amino-*N*-(5-cyanoindan-2-yl)-4-methoxybenzamide **4** as a white crystalline product. mp: 193–194ºC. ^{1}H NMR (DMSO-d6), δ: 2.93–3.02 (m, 2H), 3.22–3.30 (m, 2H), 3.68 (s, 3H), 4.65 (m, 1H), 6.07 (dd, 1H, ^{3}J 8.8 Hz, ^{4}J 2.5 Hz), 6.21 (d, 1H, ^{4}J 2.5 Hz), 6.61 (br. s, 2H), 7.42 (d, 1H, ^{3}J 7.8 Hz), 7.45 (d, 1H, ^{3}J 8.8 Hz), 7.60 (dd, 1H, ^{3}J 7.8 Hz, ^{4}J 1.3 Hz), 7.67 (br. s, 1H), 8.21 (d, 1H, ^{3}J 6.7 Hz). ^{13}C NMR (DMSO-d6), δ: 38.64, 39.22, 50.04, 54.82, 99.33, 102.12, 107.52, 109.03, 119.41, 125.66, 128.09, 130.01, 130.65, 143.23, 147.98, 152.00, 162.10, 168.73. HRMS (ESI), m/z: 308.1395 (calc. $C_{18}H_{17}N_3O_2$ $[M+H]^+$, m/z: 308.1394).

*2-Amino-N-[5-(aminomethyl)indan-2-yl]-4-methoxybenzamide hydrochloride (**5a**)*. A mixture of 2-amino-*N*-(5-cyanoindan-2-yl)-4-methoxybenzamide **4** (110 mg, 0.356 mmol), 10% Pd/C (40 mg, 10 mol. %) and HCl_{conc} (ω=35%, 100 μL) in EtOH (3 mL) was placed into a glass autoclave and hydrogen was passed through (p = 5 atm) while stirring for 8 hours until the initial nitrile disappeared (control by TLC, R_f = 0.72 in the $CHCl_3$/EtOH (20:1) system). The reaction mixture was filtered through celite, washed with EtOH, and the solvent was distilled off. The resulting product was purified by flash chromatography (eluents EtOH and EtOH/NH_3 (20:1)). This yielded 112 mg (0.322 mmol, 90%) of 2-amino-*N*-[5-(aminomethyl)indan-2-yl]-4-methoxybenzamide hydrochloride **5a** as a white crystalline product. mp: >250ºC. ^{1}H NMR (DMSO-d6), δ: 2.98 (br. s, 2H), 3.13 (br. s, 2H), 3.71 (s, 3H), 3.89 (s, 2H), 4.62 (br. s, 1H), 5.50 (br. s, 3H), 6.52 (br. s, 1H), 6.65 (s, 1H), 7.21–7.32 (m, 3H), 7.72 (br. s, 1H), 8.56 (br. s, 2H), 8.73 (s, 1H). ^{13}C NMR (DMSO-d6), δ: 38.18, 38.39, 41.98, 50.41, 55.33, 104.92, 107.10, 113.03, 124.31, 124.92, 127.16, 130.25, 131.96, 132.02, 141.44, 142.58, 161.46, 167.11. HRMS (ESI), m/z: 312.1710 (calc. $C_{18}H_{21}N_3O_2$ $[M+H]^+$, m/z: 312.1707).

*2-Amino-N-[5-(aminomethyl)indan-2-yl]-4-methoxybenzamide (**5b**)*. A 20% aqueous solution of KOH was added to a solution of 2-amino-*N*-[5-(aminomethyl)indan-2-yl]-4-methoxybenzamide hydrochloride **5a** (86 mg, 0.247 mmol) in distilled water (pH 10). The resulting mixture was extracted with CH_2Cl_2, the combined organic phases were dried over anhydrous Na_2SO_4, then filtered and the solvent was distilled off. This yielded 77 mg (0.247 mmol, quantitative yield) of 2-amino-*N*-[5-(aminomethyl)indan-2-yl]-4-methoxybenzamide **5b** as a white solid. The resulting product was used for the next step without further purification and identification.

*2-Amino-N-{5-[(1,11-dimethyl-4,8,12-trioxo-3,6,9-triazatricyclo[7.3.1.1^{3,11}]tetradecan-6-yl)methyl]indan-2-yl}-4-methoxybenzamide (**1**).* 2-Amino-*N*-[5-(aminomethyl)indan-2-yl]-4-methoxybenzamide **5b** (77 mg, 0.247 mmol) was dissolved in *N*-methyl-2-pyrrolidone (11 mL), then K_2CO_3 (345 mg, 2.50 mmol) and 3,7-bis(chloroacetyl)-1,5-dimethyl-3,7-diazabicyclo[3.3.1]nonan-9-one **6** (88 mg, 0.274 mmol) were added. The reaction mixture was stirred under heating at 70 °C for 23 hours. Then the reaction mixture was cooled to room temperature and filtered, the solvent was distilled off with an oil pump. The solid residue was treated with Et_2O and filtered off. The resulting product was purified by column chromatography (eluents $CHCl_3$, $CHCl_3$/EtOH (100:1) and $CHCl_3$/EtOH (50:1)). This yielded 62 mg (0.111 mmol, 45%) of pure 2-amino-*N*-{5-[(1,11-dimethyl-4,8,12-trioxo-3,6,9-triazatricyclo[7.3.1.1^{3,11}]tetradecan-6-yl)methyl]indan-2-yl}-4-methoxybenzamide **1** as a white crystalline product. mp: 245–247°C. ^{1}H NMR (CD_3OD), δ: 0.96 (s, 3H), 1.07 (s, 3H), 2.80–2.84 (m, 2H), 2.95–3.06 (m, 6H), 3.29–3.35 (m, 2H), 3.64 (s, 2H), 3.75 (s, 3H), 3.95 (d, 2H, ^{2}J 13.8 Hz), 4.73–4.79 (m, 3H), 4.94–5.00 (m, 2H), 6.19 (dd, 1H, ^{3}J 8.8 Hz, ^{4}J 2.5 Hz), 6.28 (d, 1H, ^{4}J 2.5 Hz), 7.23 (d, 1H, ^{3}J 7.5 Hz), 7.27 (d, 1H, ^{3}J 7.5 Hz), 7.32 (s, 1H), 7.39 (d, 1H, ^{3}J 8.8 Hz). ^{13}C NMR (CD_3OD), δ: 14.22, 14.71, 38.06, 38.34, 44.52, 44.80, 50.58, 53.58, 53.82, 54.53, 59.32, 60.89, 100.85, 104.13, 109.57, 123.93, 125.85, 128.18, 129.12, 134.25, 141.00, 141.43, 158.34, 162.53, 169.07, 169.54, 210.04. HRMS (ESI), m/z: 560.2857 (calc. $C_{31}H_{37}N_5O_5$ $[M+H]^+$, m/z: 560.2867).

2. Spectral data

^{1}H NMR spectrum of 2-amino-*N*-(5-cyanoindan-2-yl)-4-methoxybenzamide (**4**)

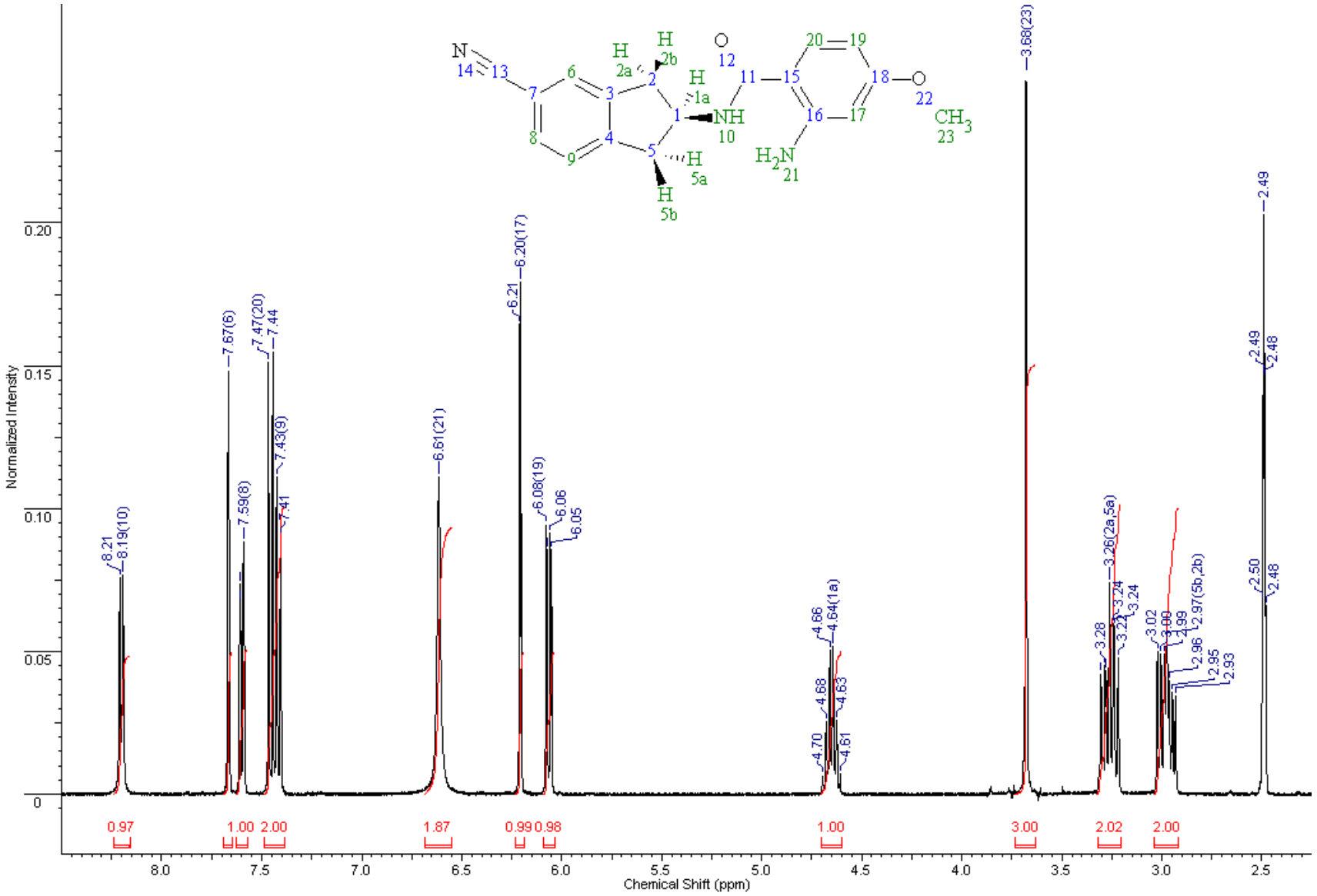

^{13}C NMR spectrum of 2-amino-*N*-(5-cyanoindan-2-yl)-4-methoxybenzamide (**4**)

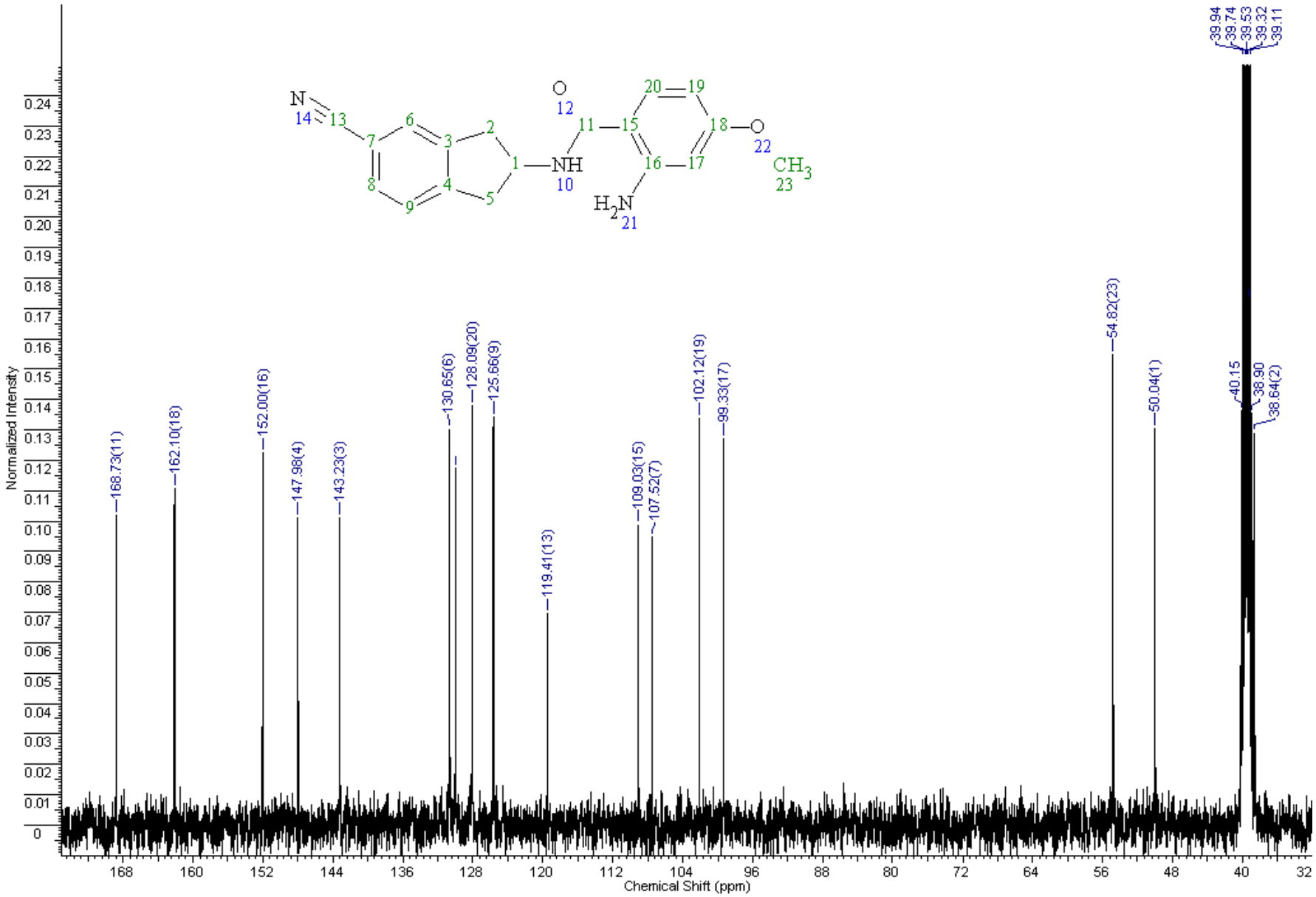

[1]H NMR spectrum of 2-amino-*N*-[5-(aminomethyl)indan-2-yl]-4-methoxybenzamide hydrochloride (**5a**)

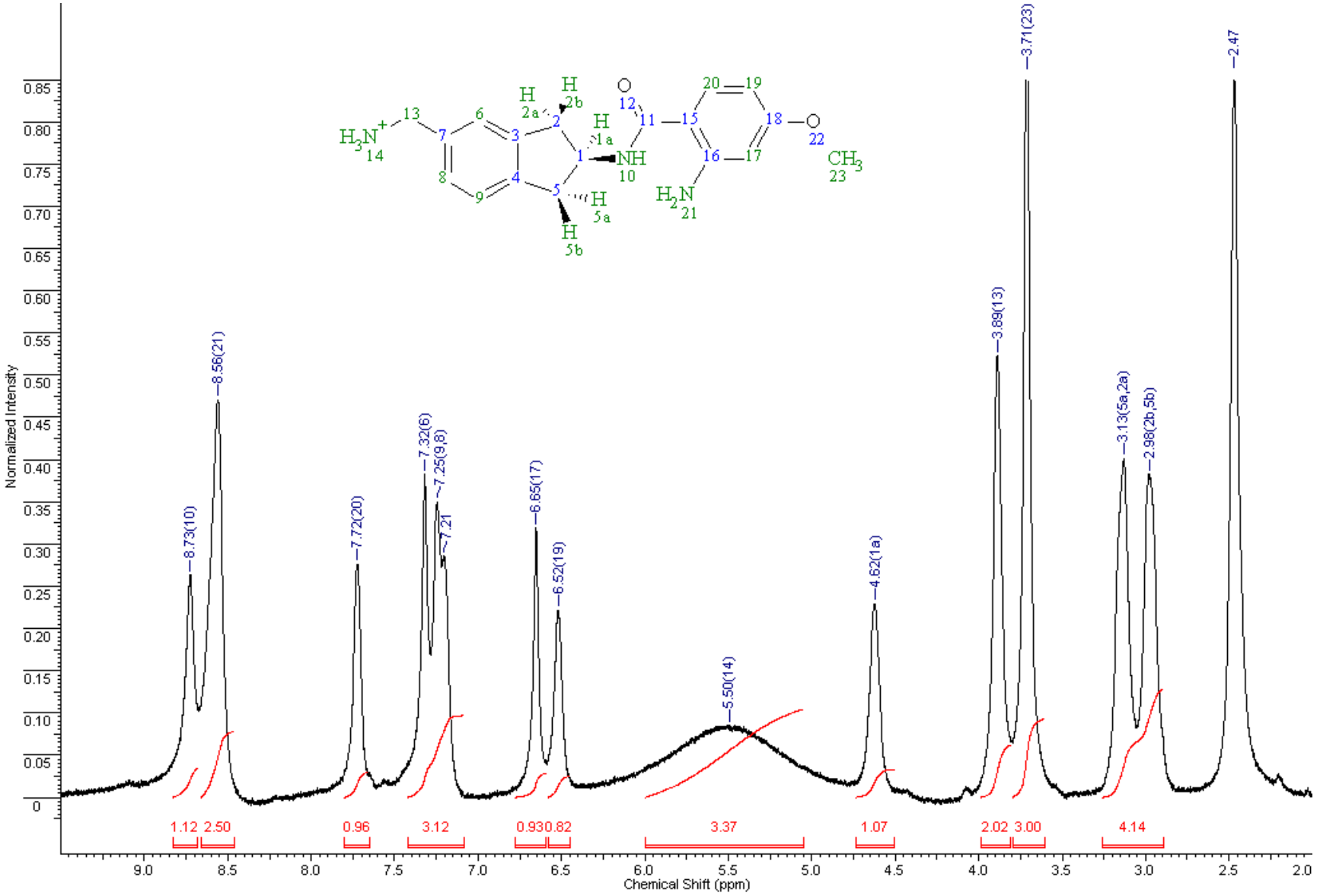

^{13}C NMR spectrum of 2-amino-*N*-[5-(aminomethyl)indan-2-yl]-4-methoxybenzamide hydrochloride (**5a**)

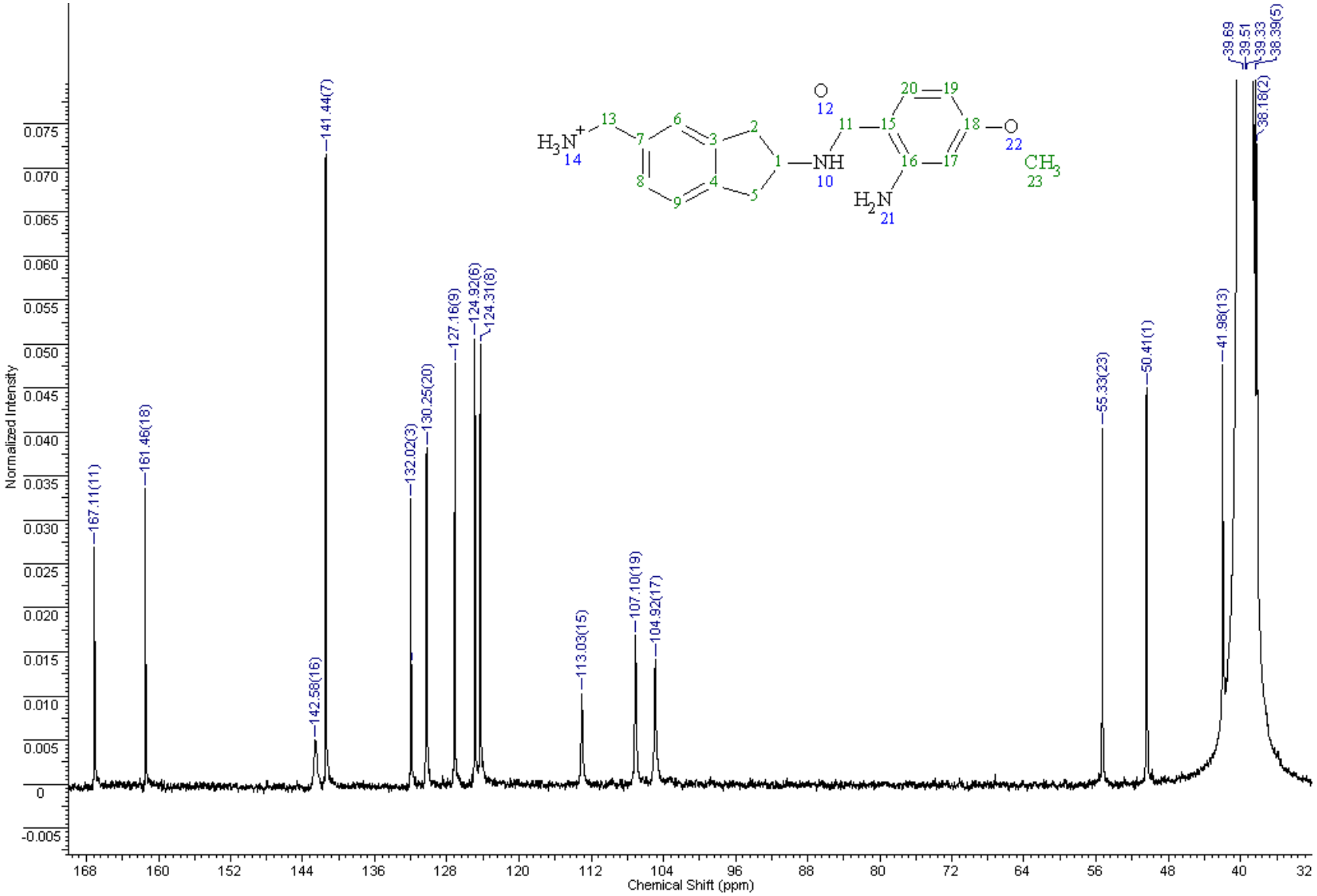

^{1}H NMR spectrum of 2-amino-*N*-{5-[(1,11-dimethyl-4,8,12-trioxo-3,6,9-triazatricyclo[7.3.1.1^{3,11}]tetradecan-6-yl)methyl]indan-2-yl}-4-methoxybenzamide (**1**)

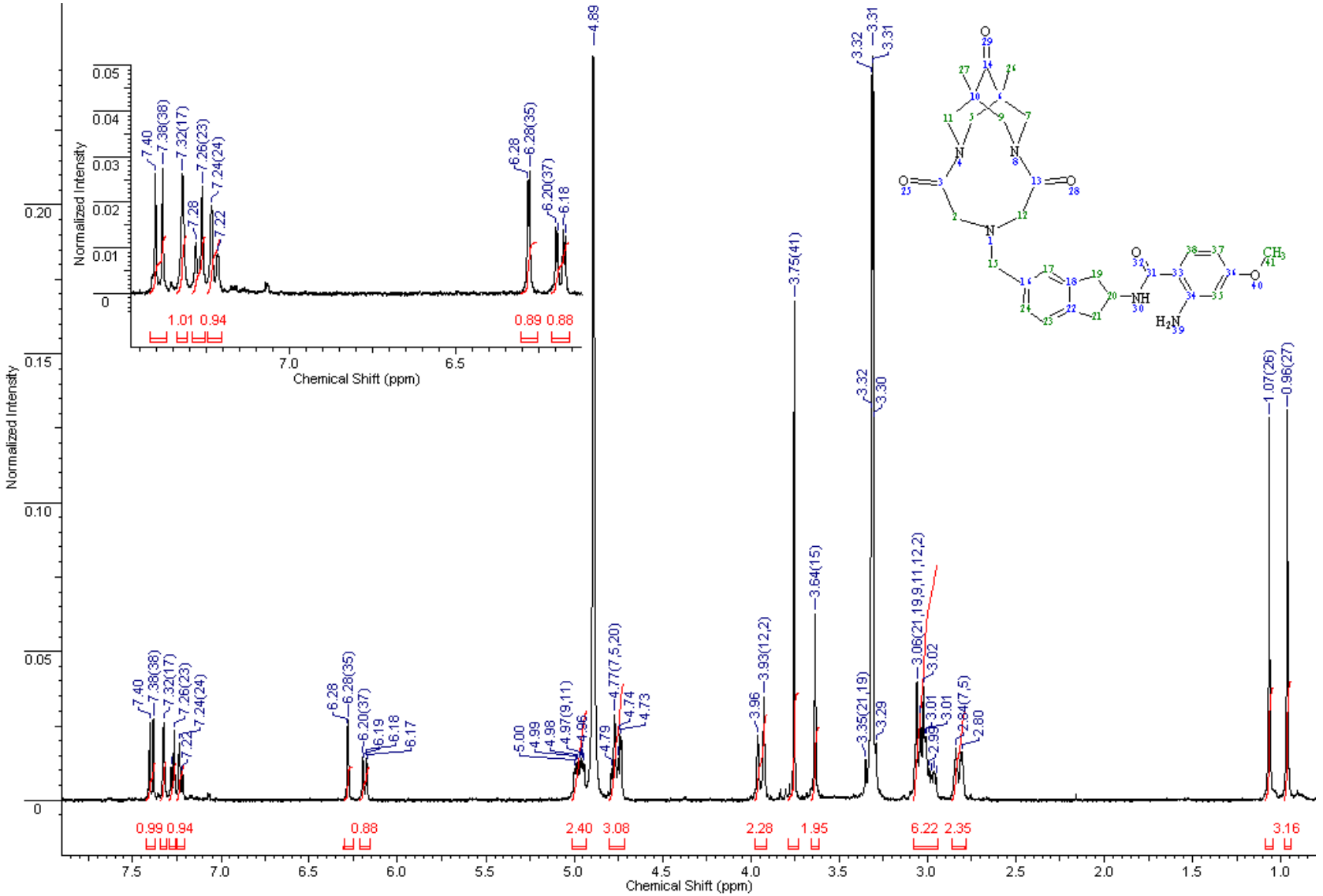

^{13}C NMR spectrum of 2-amino-*N*-{5-[(1,11-dimethyl-4,8,12-trioxo-3,6,9-triazatricyclo[7.3.1.1^{3,11}]tetradecan-6-yl)methyl]indan-2-yl}-4-methoxybenzamide (**1**)

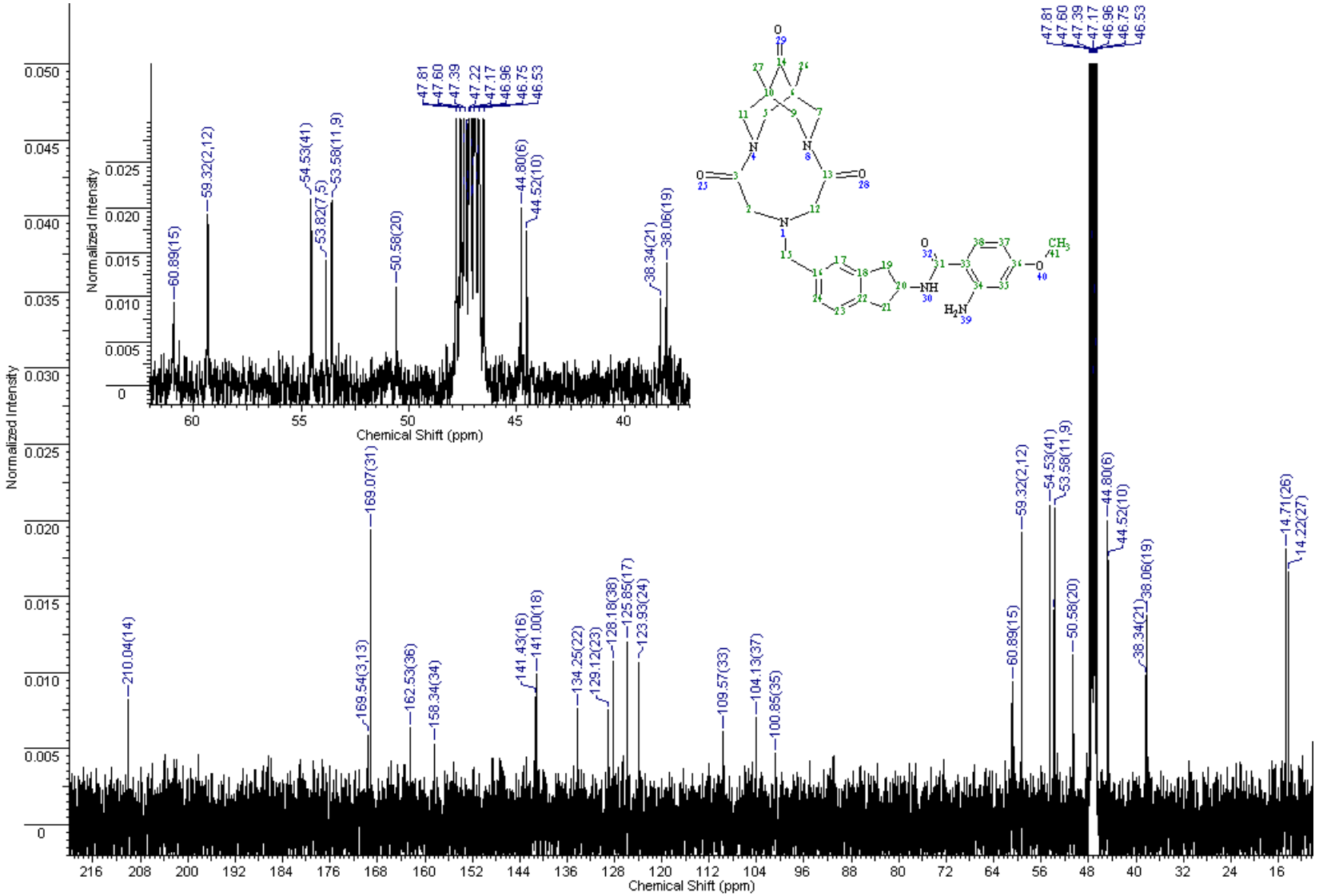

HRMS data for 2-amino-*N*-{5-[(1,11-dimethyl-4,8,12-trioxo-3,6,9-triazatricyclo[7.3.1.1^{3,11}]tetradecan-6-yl)methyl]indan-2-yl}-4-methoxybenzamide (**1**)

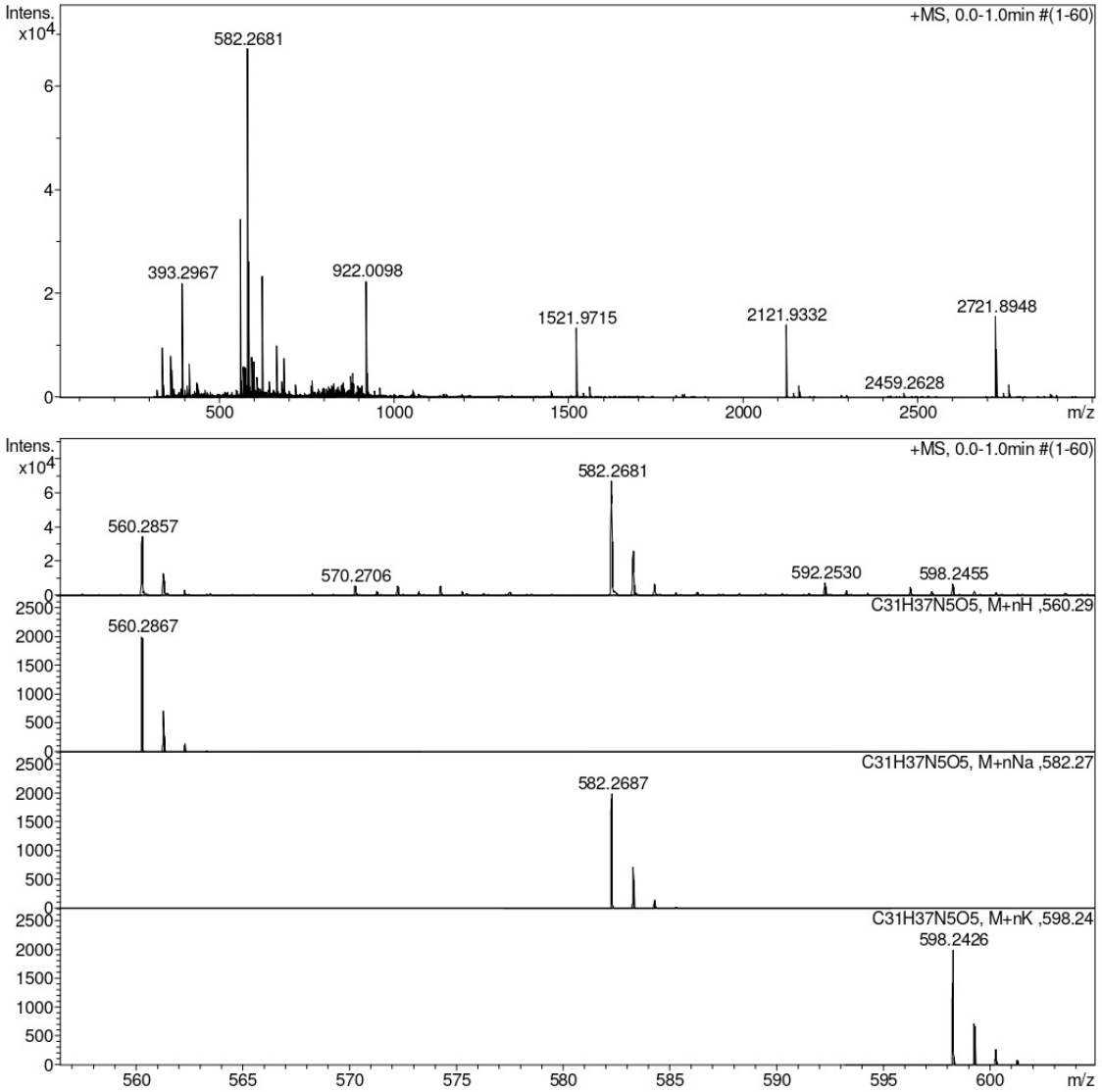

3. Electrophysiological studies

In vitro electrophysiological experiments were carried out using a patch clamp technique with local fixation of potential as described earlier.[S1,S2] Freshly isolated single Purkinje neurons from the cerebellum of 12–15 day old Wistar rats were used as a test system. Transmembrane currents were induced by the activation of AMPA receptors with a solution of their partial agonist kainic acid using fast superfusion of solutions, wherein 30 μL of the agonist buffer (the agonist concentration was varied in the range of 10^{-6}–10^{-4} M) were added to the constant flow of the neuron-washing buffer. The applications for control and each compound concentration were done in triplicate. The transmembrane currents for individual neurons were recorded using 2.5–5.5 MΩ borosilicate microelectrodes in a whole-cell configuration with an EPC-9 device from HEKA, Germany. The data were processed by a Pulsfit program from HEKA, Germany.

The study was conducted according to the guidelines of the Declaration of Helsinki and approved by the Institutional Animal Review Board of IPAC RAS.

4. Molecular modeling

The structure of the dimeric ligand-binding domain of the rat GluA2 AMPA receptor was obtained from the Protein Data Bank (PDB: 4FAT).[S3] Upon removal of ions and small molecules (except the two bound glutamate agonist molecules), the protein was allowed to relax during molecular dynamics simulation for 100 ns (see below for the simulation protocol). The most frequently occurring structure was identified by clustering of the frames in the stable part of the trajectory (40–100 ns). The ligand structures were converted to 3D and preoptimized in the MMFF94 force field using Avogadro 1.2.0 software,[S4] and then the ligand and protein structures were prepared for molecular docking using AutoDock Tools 1.5.6 software.[S5] Molecular docking into the positive allosteric modulator binding site was performed with AutoDock Vina 1.1.2 software[S6] (grid box size 22 Å × 29 Å × 40 Å, exhaustiveness = 16). The pose with the best scoring function value and ligand position was selected and the complex model was built using the UCSF Chimera 1.15 software.[S7]

The molecular dynamics simulations were performed using the CHARMM36 / CGenFF 4.6 force field[S8,S9] in the GROMACS 2024.3 software.[S10] The initial models of the systems were built using the Ligand Reader & Modeler and Solution Builder modules of the CHARMM-GUI web service.[S11,S12] The protein molecule was inserted into a rectangular periodic boundary box of water in the TIP3P model; the distance from the protein to the box border was no less than 10 Å. Individual randomly selected water molecules were replaced with potassium and chlorine ions to ensure electrical neutrality of the system and the total concentration of KCl about 0.15 M. For each system, the molecular mechanics minimization (up to 5000 steps) was performed on the CPU, followed by equilibration for 125 ps with integration timestep of 1 fs at the temperature of 300 K and constant volume using the v-rescale thermostat on the NVIDIA GeForce RTX 3080 GPU. The production simulation was performed on the GPU with integration timestep of 2 fs at the temperature of 300 K and the constant pressure of 1 bar using the v-rescale thermostat and the C-rescale barostat. The hydrogen atom movements were constrained using the LINCS algorithm. For the analysis and visualization of the results, the cpptraj software[S13] in the AmberTools 22 package[S14] and UCSF Chimera were used.

The binding free energies were estimated over the stable portion of the trajectories (last 20 ns, 101 frames at 200 ps interval) using the MM/GBSA approach implemented in the gmx_MMPBSA 1.6.1 software.[S15,S16] The internal dielectric constant $\varepsilon = 4$ and the Interaction Entropy model for the conformation entropy contribution were used. Values are listed as Mean ± Standard Error of Mean.

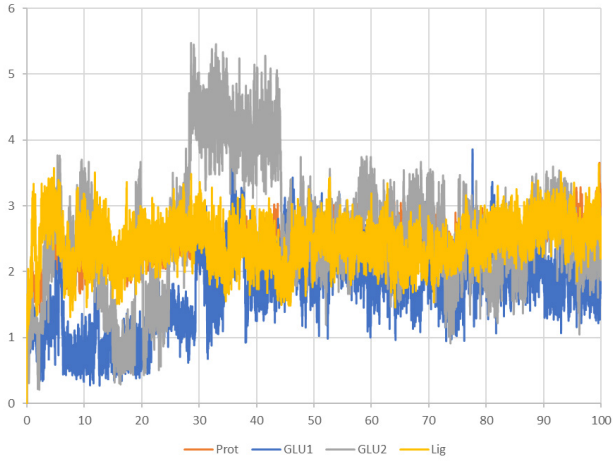

Figure S1. RMSD plots of the protein, glutamate, and ligand heavy atoms for compound **1** (S isomer) during molecular dynamics simulations of the modulator complex with the dimeric ligand binding domain of the GluA2 AMPA receptor (RMSD, Å; Time, ns).

References

S1 M. I. Lavrov, D. S. Karlov, T. A. Voronina, V. V. Grigoriev, A. A. Ustyugov, S. O. Bachurin and V. A. Palyulin, *Mol. Neurobiol.*, 2020, **57**, 191.

S2 N. S. Temnyakova, D. A. Vasilenko, M. I. Lavrov, D. S. Karlov, Y. K. Grishin, V. L. Zamoyski, V. V. Grigoriev, E. B. Averina and V. A. Palyulin, *Mendeleev Comm.*, 2021, **31**, 216.

S3 J. E. Harms, M. Benveniste, J. K. F. Maclean, K. M. Partin and C. Jamieson, *Neuropharmacology*, 2013, **64**, 45.

S4 M. D. Hanwell, D. E. Curtis, D. C. Lonie, T. Vandermeersch, E. Zurek and G. R. Hutchison, *J. Cheminform.*, 2012, **4**, 17.

S5 G. M. Morris, R. Huey, W. Lindstrom, M. F. Sanner, R. K. Belew, D. S. Goodsell and A. J. Olson, *J. Comput. Chem.*, 2009, **30**, 2785.

S6 O. Trott and A. J. Olson, *J. Comput. Chem.*, 2010, **31**, 455.

S7 E. F. Pettersen, T. D. Goddard, C. C. Huang, G. S. Couch, D. M. Greenblatt, E. C. Meng and T. E. Ferrin, *J. Comput. Chem.*, 2004, **25**, 1605.

S8 K. Vanommeslaeghe, E. Hatcher, C. Acharya, S. Kundu, S. Zhong, J. Shim, E. Darian, O. Guvench, P. Lopes, I. Vorobyov and A. D. Mackerell, *J. Comput. Chem.*, 2010, **31**, 671.

S9 J. Huang and A. D. MacKerell, *J. Comput. Chem.*, 2013, **34**, 2135.

S10 M. J. Abraham, T. Murtola, R. Schulz, S. Páll, J. C. Smith, B. Hess and E. Lindahl, *SoftwareX*, 2015, **1–2**, 19.

S11 S. Jo, T. Kim, V. G. Iyer and W. Im, *J. Comput. Chem.*, 2008, **29**, 1859.

S12 J. Lee, X. Cheng, J. M. Swails, M. S. Yeom, P. K. Eastman, J. A. Lemkul, S. Wei, J. Buckner, J. C. Jeong, Y. Qi, S. Jo, V. S. Pande, D. A. Case, C. L. Brooks, A. D. MacKerell, J. B. Klauda and W. Im, *J. Chem. Theory Comput.*, 2016, **12**, 405.

S13 D. R. Roe and T. E. Cheatham, *J. Chem. Theory Comput.*, 2013, **9**, 3084.

S14 R. Salomon-Ferrer, D. A. Case and R. C. Walker, *WIREs Comput. Mol. Sci.*, 2013, **3**, 198.

S15 M. S. Valdés-Tresanco, M. E. Valdés-Tresanco, P. A. Valiente and E. Moreno, *J. Chem. Theory Comput.*, 2021, **17**, 6281.

S16 B. R. Miller, T. D. McGee, J. M. Swails, N. Homeyer, H. Gohlke and A. E. Roitberg, *J. Chem. Theory Comput.*, 2012, **8**, 3314.